Horizon 2020 Programme

METIS

Research and Innovation Action (RIA)

This project has received funding from the European Union's Horizon 2020 research and innovation programme under grant agreement No 945121

Start date : 2020-09-01 Duration : 57 Months

Stochastic ground motion simulation for METIS case study - model calibration and database

Authors : Mrs. Luis ALVAREZ-SANCHEZ (EDF), Irmela Zentner (EDF R&D)

METIS - Contract Number: 945121

Project officer: Katerina PTACKOVA

Document title	Stochastic ground motion simulation for METIS case study - model calibration and database
Author(s)	Mrs. Luis ALVAREZ-SANCHEZ, Irmela Zentner (EDF R&D)
Number of pages	44
Document type	Deliverable
Work Package	WP4
Document number	D4.2
Issued by	EDF
Date of completion	2024-06-27 09:22:07
Dissemination level	Public

Summary

This report summarizes the calibration of a 3D stochastic ground motion simulation methodology, and the simulation of a database of synthetic ground motions for the METIS case study site, located in central Italy. The document comprises of several sections, first, a description of the herein considered ground motion simulation model is presented. Next, the calibration of the ground motion simulation model is described and finally, the simulated database is presented.

Approval

Date	By
2024-09-20 15:03:03	Dr. Marco PAGANI (GEM)
2024-09-20 16:25:30	Dr. Irmela ZENTNER (EDF)

METIS

Seismic Risk Assessment
for Nuclear Safety

Research & Innovation Action

NFRP-2019-2020

Methodologies for physics-based simulation of ground motion

Simulated database for METIS case study

Version N°2

Authors:

Luis Alvarez-Sanchez (EDF R&D)

Irmela Zentner (EDF R&D)

This project has received funding from the Horizon 2020 programme under grant agreement n°945121. The content of this presentation reflects only the author's view. The European Commission is not responsible for any use that may be made of the information it contains.

Disclaimer

The content of this deliverable reflects only the author's view. The European Commission is not responsible for any use that may be made of the information it contains.

Document Information

Grant agreement	945121
Project title	Methods And Tools Innovations For Seismic Risk Assessment
Project acronym	METIS
Project coordinator	Dr. Irmela Zentner, EDF
Project duration	1st September 2020 – 31st August 2024 (48 months)
Related work package	WP 4 – Seismic hazard
Related task(s)	Task 4.5 – Simulation of Strong Ground Motion on Bedrock
Lead organisation	EDF R&D
Contributing partner(s)	EDF
Dissemination level	open

History

Version	Submitted by	Reviewed by	Date	Comments
N°1	Luis Alvarez-Sanchez	Ssu-Ting Lai (GFZ)	03/05/2024	
N°2	Luis Alvarez-Sanchez		17/06/24	

Table of Contents

List of figures

Abbreviations and Acronyms

Acronym	Description
IA	Arias Intensity
$A^{w}{}_{i}(r_i, f)$	Attenuation for wave type 'w', source-receiver distance 'r' for sub fault 'i' and frequency 'f'
$C^{w}{}_{i_d}$	Scaling constant for sub fault 'i', component 'd' and wave type 'w'
CMS	Conditional Mean Spectrum
CS	Conditional Spectra
$Ds_{5\text{-}95}$	duration between the instants where 5% and 95% of the Arias Intensity
e	Parameter indicating the peak in the Saragoni-Hart modulating function
ESM	European Strong Ground Motion database
f	frequency
FAS	Fourier Amplitude Spectrum
f_{Tgm}	Factor modelling the elongation in the Saragoni-Hart modulating function
GM	Geometrical Mean of the horizontal components
GMMs	Ground Motion Models
IM	Intensity Measure
M_w	Moment Magnitude
M_0	source seismic moment
N_{IM}	Number of Intensity Measures considered in the calibration procedure
N_{rec}	Number of records considered in the calibration procedure
PGA	Peak Ground Acceleration
PRA	Probabilistic Risk Assessment
PSA	Pseudo Spectral Acceleration
PSHA	Probabilistic Seismic Hazard Assessment

r	source-receiver distance
R_{hyp}	Hypocentral distance
R_{jb}	Joyner Boore distance
PSA_{GM}	Pseudo Spectral acceleration of the Geometrical Mean of the Horizontal components
SDB	Simulated Database
SFs	Scaling Factors
SGMSM	Stochastic Ground Motion Simulation Method
SSEs	Sum of Squared Errors
$S^{w}{}_{i}(f)$	Source spectrum for wave type 'w'
S_0	white noise with normalized power spectral density
T_{gm}	Duration of the ground motion for computation
T^*	Conditioning period
Q	Quality factor
U	mean simulated ground motion spectrum
Vs30	Average shear wave propagation velocity of the upper 30 m
w	Wave type (S or P)
w_j	Weighting factor for IM 'j'
ω	Saragoni-Hart modulating function
$Z^{w}{}_{i_d}(f)$	Site specific effects for wave type 'w' , sub fault 'i' , component 'd' and frequency 'f'
$\Delta\sigma$	Stress drop (Bar)
κ_{SRG}	High-frequency attenuation parameter
η	Parameter indicating the attenuation in the Saragoni-Hart modulating function
ZPA	Zero Period Acceleration

Summary

This report summarizes the calibration of a 3D stochastic ground motion simulation methodology, and the simulation of a database of synthetic ground motions for the METIS case study site, located in central Italy.

The document comprises of several sections, first, a description of the herein considered ground motion simulation model is presented. Next, the calibration of the ground motion simulation model is described and finally, the simulated database is presented.

Keywords

Simulated ground motions, calibration, ground motion database.

Preamble

The goal of the METIS project is to improve existing seismic risk assessment tools and methodologies for nuclear safety. The project is organized in different work groups or "packages" also referred to as WP, targeting different steps in the chain of seismic risk assessment. Specifically, this report was developed within WP4 – Seismic Hazard, under subtask 4.5 – Simulation of Strong Ground Motion on Bedrock.

A case study was defined to assess the studied tools and methodologies. The case study corresponds to the Zaporizhzhia Nuclear Power Plant (ZNPP), and a site located on the coast of Tuscany, Italy. This hybrid case study corresponds to a compromise between the consideration of a real nuclear facility, located at an area with a more important seismic observations for the development of hazard models.

One of the objectives of WP4 is to evaluate the possibility to use synthetic earthquake ground motion, simulated at a reference rock-site, as input for site-specific seismic risk assessment. To achieve this objective, contributors of WP4 identified a series of available ground motion simulation methodologies and discussed their advantages and disadvantages towards and application such as that envisioned within the context of the METIS project. Deliverable D4.3 summarises these comparisons. In the end, two ground motion simulation methodologies were considered for the METIS case study, the 3D stochastic ground motion simulation methodology and the recorded ground motions corrected for the site terms, described in sections 3.3 and 3.4 of deliverable D4.3, respectively. This document summarizes the methodology and results obtained in the simulation of the databased of synthetic ground motions considering the former of these ground motion simulation methodologies.

Introduction

In the context of probabilistic seismic risk assessment (PRA) seismic load needs to be defined in agreement with safety requirements and the hazard at a site. For transient response analysis, ground motions acceleration time histories are required. Databases of these earthquake ground motions, however, are often scarce and are incomplete for a wide range of scenarios of interest. In addition, only fewer records are available for rock sites. In fact, most strong-motion databases contain earthquake recordings of stations installed on soil or soft-rock sites, while very few stations are on hard-rock sites. These ground motions are needed for various applications, moreover, the definition of the features of the "rock" site also depend in the intended application, (Lanzano, Felicetta, Pacor, Spallarossa, & Traversa, 2022). One of the most typical applications, however, is that of the definition of a reference rock (Steidl, Tumarkin, & Archuleta, 1996), i.e., with a flat/unamplified response over a frequency range of engineering interest , where site-effects are to be added subsequently according to soil response analysis.

To circumvent the shortage of recorded ground motions at reference rock sites, researchers and practitioners have considered recordings from both rock and soil sites, and from simulated ground motions. Studies such as Garcia de Quevedo Inaritu et al., (2023), and Alvarez et al., (2023), developed within the framework of the METIS project, have looked at the implications of such considerations in terms of risk analysis of single structures.

To explore the potential of simulated ground motions, the METIS project set the goal to develop and test methods to generate databases of synthetic ground motion time histories on bedrock. To do so, WP4 has studied series of ground motion simulation methodologies summarized in Deliverable D4.3. One of such methodologies is the 3D stochastic ground motion simulation methodology originally presented by Otarola et al., (2016) and Ruiz et al., (2019), and later modified by Alvarez (2022). This ground motion simulation technique builds over other stochastic methods such as those presented in Boore (1983), Boore and Atkinson (1997) and Motazedian et al., (2005), by incorporating a model for the full body wave field spectra (i.e., P, SV and SH-waves). Another advantage of this technique is the physical meaning of the parameters used in the construction of the synthetic ground motions, this feature allows a direct link between seismicity recorded at the region and subsequent simulations, using source and path terms consistent with the ones used to compute seismic hazard. Finally, applications such as that presented in Alvarez (2022) have demonstrated the compatibility of the technique for the generation of databases of simulated ground motions to be used for earthquake response assessment.

This report presents the implementation of the 3D stochastic ground motion simulation methodology for the purpose of the METIS case study. The first section of this document introduces the ground motion simulation technique. Next, a set of regional recorded ground motions is introduced for its use as reference in the derivation of the input parameters required for the simulation of ground motions with the herein

considered technique. Afterward, the calibration of the simulation technique is shown and assessed by comparing simulated and reference recorded ground motions in the region of the case study. Finally, the calibrated model is used to generate a database of simulated ground motions, populated with new earthquake scenarios consistent with those obtained from the disaggregation of the hazard computed for the METIS case study. This database of simulated ground motions is then contrasted with ground motion models relevant for the area of interest and used for record selection according to the methodologies developed within the METIS project. It is acknowledged that the set of input and output data used in this work are available on the METIS Zenodo community. Links to all METIS references are provided in the reference section at the end of this document.

1. Ground Motion Simulation Technique

The ground motion simulation method presented in this section, and from here on referred to as SGMSM, is a modified version of the stochastic technique introduced in Otarola & Ruiz, (2016) and Ruiz et al., (2018), and modified to include a more realistic representation of the source and the inter-frequency correlation structure of the spectral amplitudes.

The stochastic ground motion simulation method proposed in Otarola & Ruiz, (2016) and Ruiz et al., (2018) computes time histories in the frequency domain and model the Fourier Amplitude Spectrum (FAS) as a convolution of modulated noise with a random phase and a mean ground motion spectrum:

$$FAS = U(f, r, M_0)\sqrt{S_0} \quad (1)$$

Where U is the mean simulated ground motion spectrum, S_0 is the white noise with normalized power spectral density, f is the frequency, r is the source-receiver distance, and M_0 is the source seismic moment. Considering a finite-source model, where the source is discretized into an array of point-sources, time histories are constructed as the lagged summation of the individual sub faults contributions, (Atkinson et al., 2009; Beresnev & Atkinson, 1997; Motazedian & Atkinson, 2005). The definition of the mean simulated ground motion spectrum, for wave type w (P, SV, and SH), sub-source i and component d (vertical, radial, and tangential) is shown in the following equation:

$$U_i^w{}_d\left(f, r_i, M_{0_i}\right) = C^w{}_{i_d}(, M_{0_i})\, S^w{}_i(f) A^w{}_i(r_i, f) Z^w{}_{i_d}(f) \quad (2)$$

Where $\mathrm{C}^{\mathrm{w}}{}_{i_d}$ is the scaling constant, $S^w{}_i(f)$ represents the source, $A^w{}_i(r_i, f)$ the propagation (attenuation due to the path) and $\mathrm{Z}^{\mathrm{w}}{}_{i_d}(f)$ the site-specific effects component of the simulated ground motion spectrum. The full description of the formulation of each of these components can be found in Alvarez (2022).

The phase of the simulated ground motions is included by the mean of the band-limited Gaussian white noise with finite duration. The duration of the ground motion, on the other hand, is modelled considering a source related component (linked to the rise time of the assumed source model), and a propagation component (related to the elongation of the signal with respect to the distance from the source). A modulating function is applied to the white noise with the intention to include the characteristic temporal non-stationary nature of ground motion time series. The Saragoni & Hart modulating function, $\omega(t, e, \eta, t_\eta)$ (Saragoni & Hart, 1973), shown in equation (3) is often considered in stochastic simulation methods, e.g., Otarola & Ruiz (2016) and Ruiz et al., (2018), and was also considered in this study.

$$\omega(t, e, \eta, t_\eta) = a\left({}^{t}/_{t_\eta}\right)^b \exp\left(-c\left({}^{t}/_{t_\eta}\right)\right) \quad (3)$$

Where e and η are parameters defining the shape of the function, $a = exp(1)/e$, $b=-e\ln(\eta)/(1+e\cdot(\ln(e)-1)$, $c=b/e$, $t_\eta = f_{Tgm} \cdot T_{gm}$. T_{gm} is the duration of the signal for the computation of the window function, and f_{Tgm} is a factor modeling the elongation of the windows. Previous implementations of this modulating function have considered different combinations of parameters. These, however, are often adjusted for matching reference signals, e.g., Otarola & Ruiz (2016) and Ruiz et al., (2018)

The SGMSM differs from previous stochastic methods such as those considered in Beresnev & Atkinson (1997); Boore (1983), (2003); Motazedian & Atkinson (2005), not only by computing the whole body-wave spectra, but also for using a ray-like propagation of the seismic waves through a layered media (considering Snell's law to vary the incidence angle of the seismic rays coming from the source to the site). Finally, this methodology includes a postprocessing procedure to add the correlation structure between spectral amplitudes coming from the analysis of within-site residuals (Wang et al., 2019). More details on this procedure may be found in Alvarez (2022) and METIS D4.3 (Akazawa, et al., 2023).

2. METIS case study

The case study of the METIS project was defined to demonstrate the methods and tools tested within the context of the project. This case study considers a hypothetical nuclear facility located in the western coast of Tuscany. The hazard at the site of the case study was estimated by means of PSHA (Cornell, 1968), following the methodology described in Chartier et al., (2023) and for a site with an average shear wave velocity of the upper 30m (*Vs30)* of 1000 m/s. The hazard curves obtained for three different Pseudo-Spectral-Acceleration (PSA) values are shown in Figure 1.

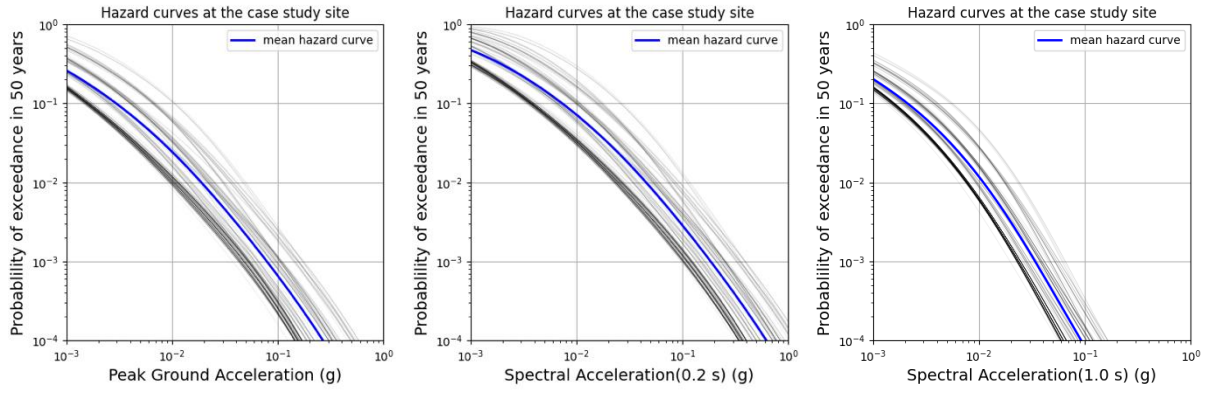

(a) (b) (c)

Figure 1: Hazard curves for spectral accelerations at three different PSA: (a) – PGA, (b) -PSA(0.2s), and (c) – PSA(1.0s). The mean hazard curve is shown in blue and the 200 individual realisations in grey, (Chartier & Rood, 2023)

Simulated ground motions were considered within the case study with the objective of providing supplementary input acceleration time histories for structural response analysis. Because acceleration time histories may theoretically be simulated at any desired location, the advantage of a database of simulated ground motions lies in the

capacity to provide the specific scenarios missing in the database of recorded ground motions.

3. Reference recorded ground motions

Regardless of the considered simulation technique, ground motions contained within the simulated database should be consistent with ground motions recorded in the region of the case study. To achieve this objective, a set of ground motions recorded at the region of interest, and selected from the ESM database, (Lanzano G, 2019), were first studied to derivate distributions of meaningful input parameters to be considered in tandem with an application specific calibration of the ground motion simulation technique.

The reference set of recorded ground motions was carefully chosen within a region of interest bounded by parallels 41° and 43.5°N and meridians 11° and 15°E. This subregion was designed to identify any local effects on spectral content and duration while ensuring a minimum of 10 earthquake records for events with magnitudes greater than 6.0 ($M_w \geq 6$). Ground motions were then categorized by their magnitude and recording site characteristics. In agreement with the hypothesis of the PSHA conducted for the site this study considers only the events with magnitudes above 4.0 ($M_w \geq 4$) and sites with Vs_{30} above 1000 m/s ($Vs_{30} \geq 1000\ m/s$). Figure 2 shows the relative location of the epicenters of the earthquake events and stations considered in this study.

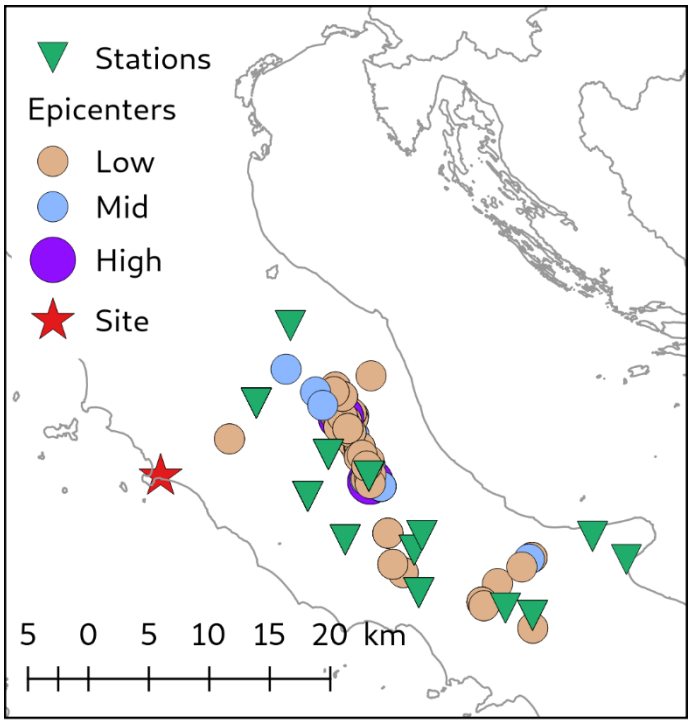

Figure 2: (a) - Locations of the epicenters (circles) and stations (triangles) of interest. The location of the site of the case study is marked with a red star. In the figure, the magnitude of the earthquakes is shown by the color of the marker, where low magnitude is considered for $4 < M_w \leq 5$, mid magnitude for $5 < M_w \leq 6$, and high magnitude for $6 < M_w$

All downloaded time histories were treated before any manipulation. The processing of the time histories consisted of the following steps:

1. Baseline correction by subtraction of the average of the time series.
2. 5% cosine tapering at the beginning and at the end of the signal.
3. Application of a band-pass (acausal) filter to eliminate the low-frequency noise and the response of the measuring instrument. This study considered Butterworth filter ($n = 3$), with a high-pass corner frequency given by the maximum between (i) the frequency at which the signal-to-noise ratio, SNR, of the motion was above the value of 3, or (ii) the interception of the FAS with a f^2 function, (Boore, On pads qnd filters: Processing strong motion data, 2005). The low-pass corner frequency of the filter was set at 24 Hz since this is the maximum frequency included in the correlation model considered within the ground motion simulation.

4. Input parameters for ground motion simulation for METIS case study

The generation pf synthetic ground motions with the SGMSM described in section 1 requires the definition of a series of parameters/models, which are: i) the parameters defining the simulated ground motion spectrum, ii) the parameters defining the duration and time modulating functions characterizing the time histories, iii) the source (geometry and slip) and finally iv) crustal models. The following sections describe each of these individual inputs as defined by the recorded ground motions in previous studies or in the literature referenced for METIS case study site (see METIS D4.6 for more detail on METIS case study on hazard and site).

4.1. Ground motion spectrum

This study considered the seismological characterization of the area of central Italy reported in Morasca et al., (2023). They presented the distributions of the input parameters used in common stochastic simulation techniques to parametrize the simulated ground motion spectrum. Their results are based on the study of more than 30000 waveforms recorded from 456 earthquakes by about 460 stations located in the proximity of the site of the METIS case study. According to Morasca et al., (2023), the studied earthquake events were characterized by two different distributions of stress drop ($\Delta\boldsymbol{\sigma}$). The first distribution was defined for events with a seismic moment ($\boldsymbol{M_0}$) below 6.4e16 N-m, and the second one for events with a seismic moment above 10e17 N-m. Equations (4) and (5) show the models obtained from the inversion of these distributions, respectively. The source spectra reported by the authors is completed with the consideration of the high-frequency attenuation function parametrized by $\boldsymbol{\kappa_{SRG}}$ and was introduced first in Anderson et al., (1984) (typically considered as part of the attenuation model, i.e., Boore (2003)). The distribution of the $\boldsymbol{\kappa_{SRG}}$ presented by the authors and the regression modelled developed as part of this study are shown in Figure 3

$$log_{10}(\Delta\sigma) = 0.380(\pm 0.063) log_{10}(M_0) - 5.748(\pm 0.972) \quad (4)$$

$$log_{10}(\Delta\sigma) = 0.088(\pm 0101) log_{10}(M_0) - 0.545(\pm 1.814) \quad (5)$$

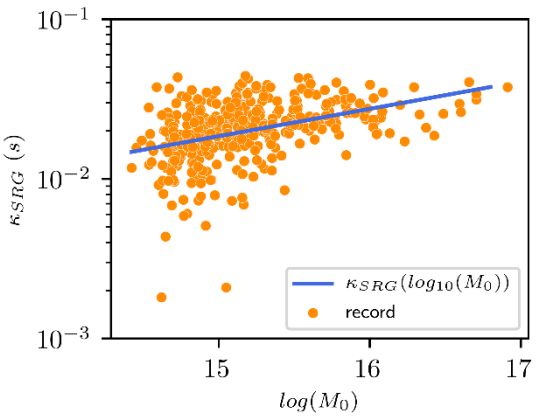

Figure 3: Distribution of the high-frequency attenuation parameter, $\boldsymbol{\kappa_{SRG}}$, as a function of Moment Magnitude (M_0); Morasca et al., (2023). The regression model shown in the figure was developed as part of this study.

Regarding the attenuation, Morasca et al., (2023) reported a bilinear geometrical attenuation function with a hinge at 70 km, as it may be seen in equation (6). Regarding the quality factor of the S-waves (Q^S) , the authors considered a function of the form $Q^S(f) = Q_0 f^M$, where $Q_0 = 247 \pm 12.8$ and $M = 0.38 \pm 0.03$.

$$G(R_{hyp}) = \begin{cases} \left(\frac{10}{R_{hyp}}\right)^{1.77} & R_{hyp} \leq 70\ km \\ \left(\frac{10}{70}\right)^{1.77} \left(\frac{70}{R_{hyp}}\right)^{0.56} & R_{hyp} > 70\ km \end{cases} \quad (6)$$

Finally, no site-effects were considered in the representation of the FAS because the objective of this application is to generate reference acceleration ground motion for site specific analysis. It is important to highlight that, according to the theory behind the Generalized Inversion technique, e.g., (Oth, Parolai, & Bindi, 2011), this calibration results in simulated ground motion spectra consistent with the station (or combination of stations) used to define the reference condition to separate source and site contributions. The combination of stations considered by the authors results in a mean Vs_{30} = 900 m/s.

4.2. Ground Motion duration

The duration of the simulated ground motions of a single sub fault (or fault model in the case of a single point source)(T_{gm}) was considered as the significant duration of the ground motion ($Ds_{5\text{-}95}$) and is defined as the duration between the instants where 5% to 95% of the Arias Intensity (IA) integrated through the time series is reached.

The definition of these durations follows the study of the reference recorded ground motions introduced in section 3. Figure 4 shows the distribution of T_{gm} vs R_{hyp} for the considered set (where each record is assumed to be generated from a point source). Also included in the Figure 4 is the median of the regressions conducted for three subsets selected based on different magnitude bins, i.e., $4 < M_w \leq 5$, $5 < M_w \leq 6$, $6 < M_w$. As shown in Figure 4, there are no significant differences in the regressions

models for the two sets characterized by the lowest magnitude bins, therefore the herein application considers two durations models, one for events with magnitude below 6.0 ($6 \geq M_w$) and shown in equation (7), and a model for events with magnitudes above 6 ($6 < M_w$) and shown in equation (8).

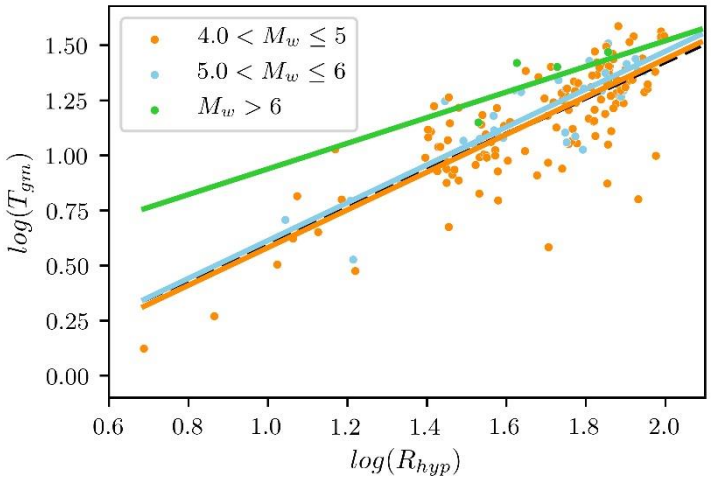

Figure 4: Distribution of the significant duration of ground motions recorded at the region of the case study.

$$log_{10}(T_{gm}) = 0.67 log_{10}(R_{hyp}) - 0.27 + N(0, 0.15) \quad (7)$$

$$log_{10}(T_{gm}) = 0.357 log_{10}(R_{hyp}) + 0.582 + U(-0.1, 0.1) \quad (8)$$

The definition of the modulating functions that shape the acceleration time history in the time domain is discussed in the upcoming sections detailing the calibration of the SGMSM.

4.3. Crustal structure

The model of the crustal structure used in this study is that of Li et al., (2017). They reported a series of layered velocity models in different regions of Italy. The models are based on the inversion of locally recorded data and include the uncertainty related to the depth and wave-propagation velocities at each layer of the model. Figure 5 shows the crust model for the herein considered region.

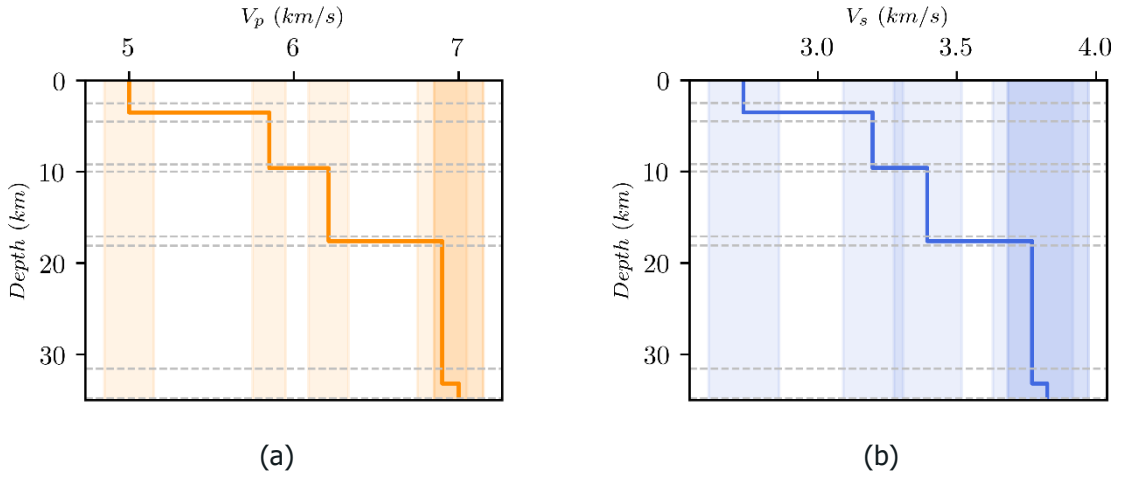

Figure 5: Regional layered model for the crust (Li et al., 2017). Wave propagation velocities of (a) – P waves, and (b) S waves. The dashed lines represent the range of variability of the depth of the interfaces and the shadowed regions are that of the propagation velocities. Darker shadowed regions simply represent the superposition of the rages of possible propagation velocities at different depths.

4.4. Source model

Each event simulated in this study was generated with a finite source model. The variability in their geometry was considered using the relationship proposed by Wells & Coopersmith (1994), where the length and width of the fault depend on the size and mechanism of the rupture. To complement the geometry of the source, each of the fault planes was oriented with dip and strike angles sampled randomly from uniform distributions varying between 10°-90° and 0°-359°, respectively. Regarding the definition of the slip distribution, this study considered the kinematic source model reported by Ruiz et al., (2011) to generate distributions of 1000 asperities uniformly distributed along the rupture surface. Finally, the propagation of the rupture in each of the conceived sources was modelled with the algorithm reported in Gallovič et al., (2016).

4.5. Calibration of the SGMSM

The characterization of the SGMSM was completed by a calibration procedure to adjust the shape of simulated acceleration time histories and the amplitude of the ground motion movement to match those of the reference recorded ground motions introduced in section 3. In the preliminary phase of this work, the lack of a site-specific parametrization for the time modulating functions, and the use of the stress drop

distributions reported in Morasca et al., (2023), led to simulated ground motions with unrealistic durations and overly large high-frequency content.

To our knowledge, there is limited available references providing guidance on the modelling of the time modulating window functions within a finite-fault context. One existing possibility is the iterative calibration procedure proposed in Alvarez (2022). The goal of this optimization process is to minimize the differences between the IMs of interest extracted from the set of reference recorded ground motions and those extracted from sets of synthetic ground motion computed with different combinations of the target modeling parameters. These are herein referred to as replicas. The parameters resulting in the closest fit between replicas and the recorded events is chosen as the optimal solution.

Same as Alvarez (2022), this study considered the proposed iterative calibration procedure to optimize the following modeling parameters including: (i) the time-modulating window parameters (i.e., e, η and f_{Tgm}) that govern the location of the peak, attenuation, and elongation of the window; and (ii) the stress drop, which defines the source. The replicas used in the calibration were constructed by generating one simulated ground motion per record in the reference recorded set using the same causative parameters, i.e., M_w, R_{hyp}, and Z_{hyp}, of the recorded ground motion. The difference in the recorded and simulated ground motions in terms of the j^{th} Intensity Measure (IM) can be defined by Equation (9).

$$\varepsilon_{ij} = ln\left(IM_{ref,_{ij}}\right) - ln\left(IM_{sim,_{ij}}\right) \quad (9)$$

Here, $IM_{ref,ij}$ and $IM_{sim,ij}$ show the corresponding values of the IMj in i^{th} pair of recorded and simulated ground motions. To find the total residual of a set of simulated ground motions, one can compute the sum of the square of the error terms obtained for multiple IMs (i.e., total of N_{IM}) and for all the records in the database, N_{rec}, according to Equation (10).

$$Error = \sum_{i=1}^{N_{rec}} \sum_{j=1}^{N_{IM}} w_j \cdot {\varepsilon_{ij}}^2 \quad (10)$$

Here, w_j represents a weighting factor allowing the prioritization of the match of IM_j $j=1,\ldots, N_{IM}$ considered in this procedure. In this study, two calibration rounds were run to target each of the specific issues at hand. First, an initial calibration round targeting the amplitude of the ground motion was conducted, here only the Peak Ground Acceleration (PGA) of the Geometrical Mean (GM) of the Horizontal components was chosen as target IM (thus setting the weighting factor to 1.0). Next, a second round of calibration was run targeting the overall shape and duration of the simulated acceleration time histories. In this round, a vector of 3 IMs was considered: $Ds_{5\text{-}95}$, $Ds_{5\text{-}75}$, *and* $Ds_{20\text{-}80}$ with weighting factors of 0.5, 0.25 and 0.25, respectively.

In this study, three different groups of ground motions were defined in recognition of the overall differences between the target IMs as a function of magnitude: low magnitude events ($4 < M_w \leq 5$), medium-magnitude events ($5 < M_w \leq 6$), and high-

magnitude events ($6 < M_w$). The optimal set of parameters for each group and calibration run was searched a total of 10 times, with each search considering a different pool of likely combinations and overall random seeds for generating simulated ground motion and sampling of input parameters. The simulation of the replicas followed an event-based approach, which means that all the simulated replicas coming from an earthquake scenario share the same source parameters, i.e., finite rupture model and source spectrum. Regarding the duration of the ground motion, each of the sub faults within the finite source model was assigned a duration based on its estimated moment magnitude (proportional to the slip of the sub fault and the total slip of the major fault) and described in detail in section 4.2.

Figure 6 shows the distributions of stress drops obtained from the calibration procedure for the three defined groups. The figure includes the histograms and regressions conducted for the deduced populations of the parameter. The results indicate that the three populations follow a log-normal distribution with similar mean and standard deviation values. These results differ with those reported in Morasca et al., (2023), who proposed significantly different distributions for events with seismic moments below 6.4e16 N-m $(M_0 < 6.4e16\ N-m)$ and above 10e17 N-m $(M_0 > 10e17\ N-m)$. These discrepancies were attributed to the differences between the SGMSM and the Brune model (Brune, 1970) conducted in Morasca et al., (2023), for regression analysis. The discrepancies are mostly important for the highest magnitude group, suggesting that differences may also be due to the consideration of a finite fault source model in the generation of the simulated ground motions. In fact, the mean value for events within the low and mid magnitude groups fairly matches that reported in Morasca et al., (2023).

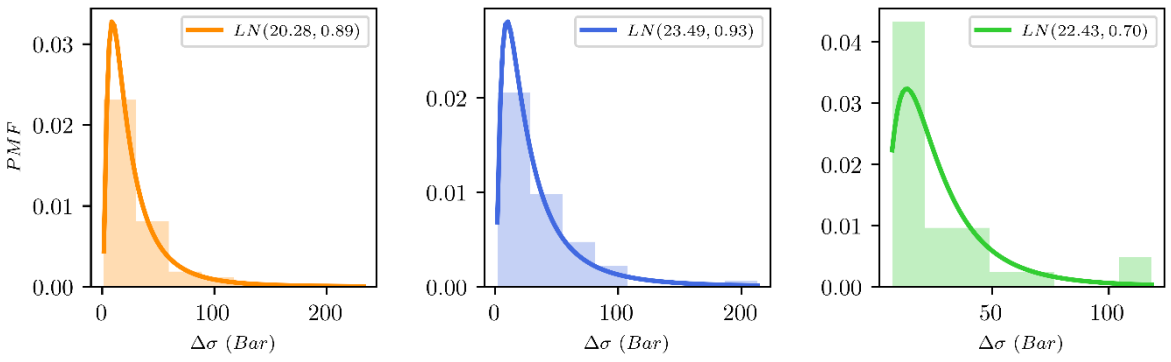

(a) (b) (c)

Figure 6: Distributions of stress drops obtained from the calibration procedure for (a) – Low, (b) – Mid, (c) – High magnitude earthquakes as defined in this report. The legend of each plot indicates the parameters of the Log Normal (LN) distribution fitted to the results, mean and logarithmic standard deviation, respectively. The Y-axis of the histograms refers to the Probability Mass Function (PMF)

The results for the elongation parameter of the modulating functions are shown in Figure 7, indicating that the deduced parameters follow similar trends for the three considered groups. This consistency suggests that the duration model described in

section 4.2 is representative of the duration of the recorded reference ground motions and indicates that the elongation of the windows could be uniformly parametrized.

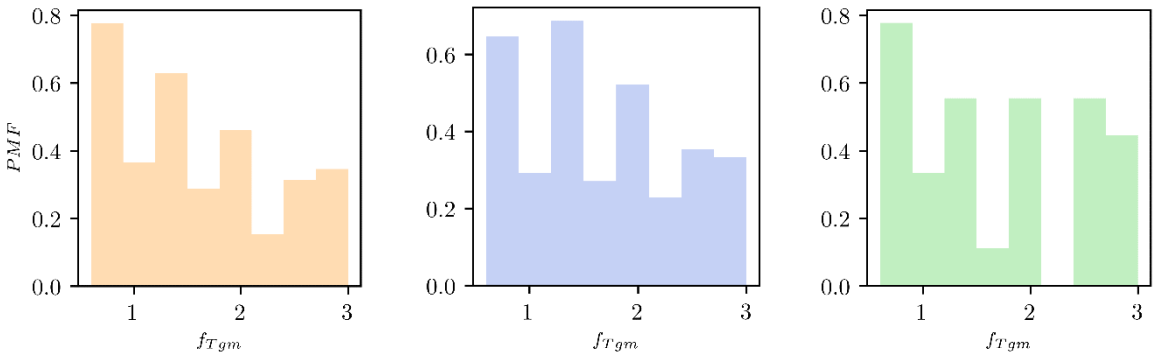

Figure 7: Distributions of f_{Tgm} from the calibration procedure for (a) low, (b) mid, (c) high magnitude earthquakes as defined in this report. The Y-axis of the histograms refers to the Probability Mass Function (PMF)

Figure 8 shows a comparison of three of the simulated acceleration time histories, or replicas, obtained for one reference recorded ground motion of the high magnitude group ($M_w = 6.0$, $R_{hyp} = 27.9\ km$). The acceleration time histories in this figure are aligned at the instant where they reach 1% of the IA ($0.01IA$). Taking a broader view across the different calibration groups, Figure 9 and Figure 10 show a comparison of several IMs considered directly or indirectly in the calibration procedure. Figure 9 indicates a good agreement between the response spectra of the geometrical mean of the horizontal components (PSA_{GM}) from recorded and synthetic replicas for the low and mid-magnitude earthquakes in terms of mean and dispersion (illustrated by the shaded area representing the space between the 16th and 84th percentiles of the distribution) and for periods of vibration up to 10s. The results obtained for the highest magnitude range, shown in Figure 9c, differ for the longest period range due to a more accentuated attenuation of the simulated ground motions. This observation is consistent with the broadly know limitation of stochastic simulation methods to represent the low-frequency content of earthquake ground motion, (Akazawa, et al., 2023). The short period content, however, shows a much more similar distribution when compared to the recorded references. Overall, these results are considered satisfactory, particularly given the matching spectral content of reference and simulated ground motions at short periods. This similarity was directly targeted during calibration procedure by searching for the distributions of stress drop resulting in matching peak ground accelerations.

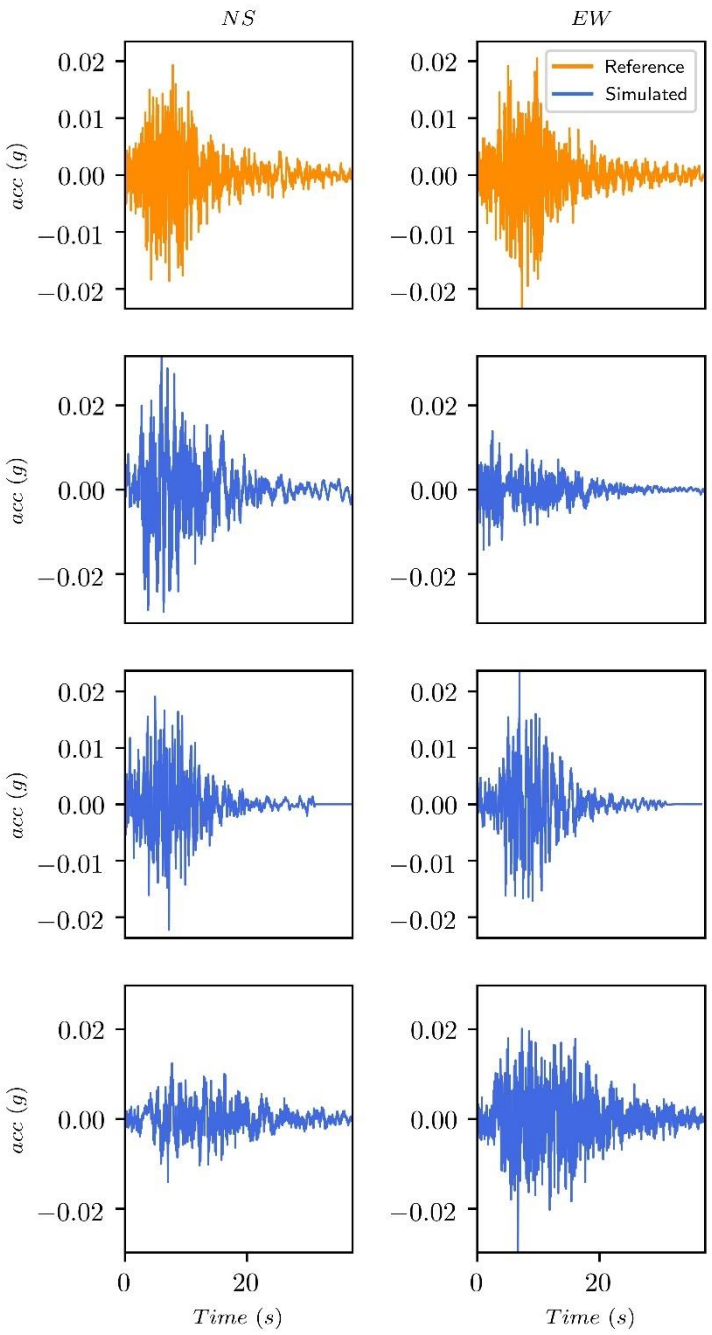

Figure 8: Comparison of three different replicas for one of the reference acceleration time histories for the high magnitude earthquakes ($M_w = 6.0$, $R_{hyp} = 27.9\ km$).

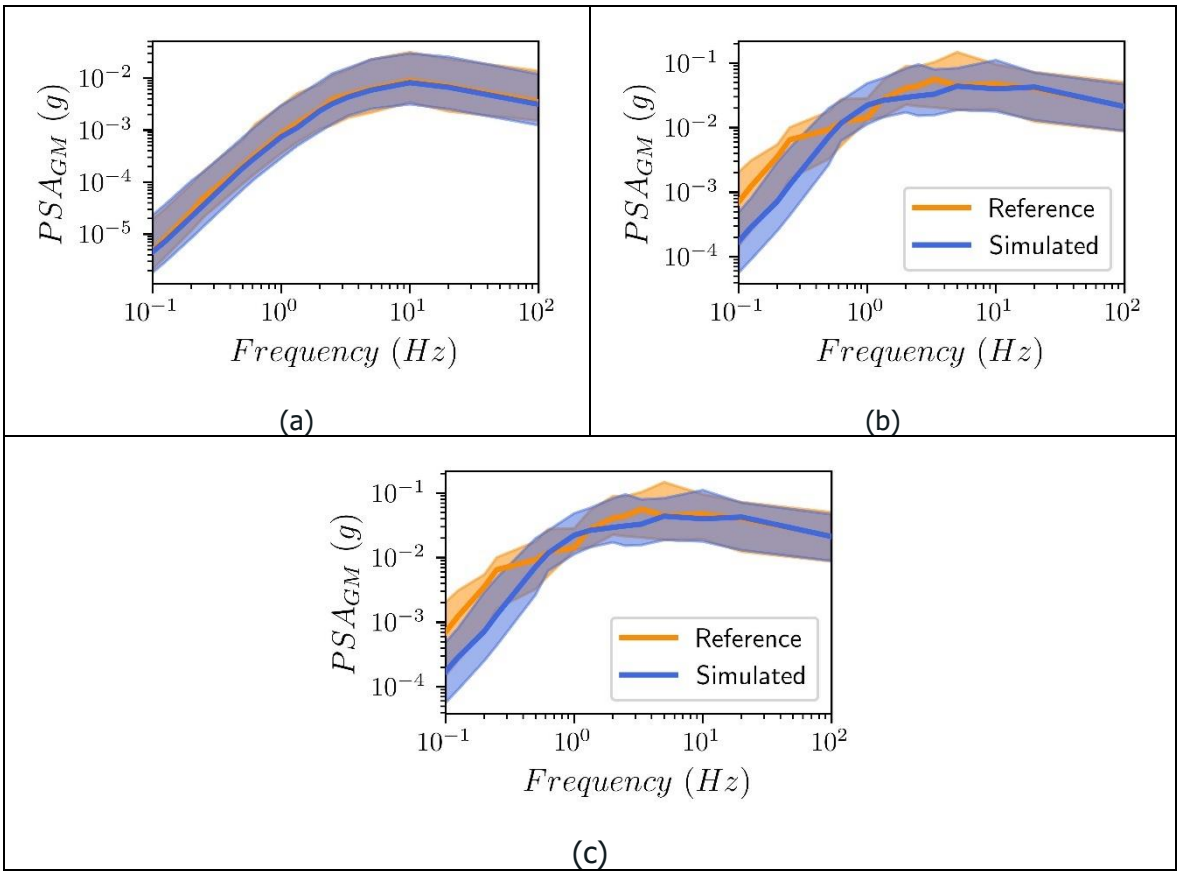

Figure 9: Comparison of response spectra of the geometrical mean of the horizontal components (PSA_{GM}) computed from the reference and synthetic ground motion generated at the end of the calibration procedure is shown for (a) low, (b) mid, and (c) high magnitude earthquakes as defined in this report.

The comparison of the significant durations ($Ds_{5\text{-}95}$, $Ds_{5\text{-}75}$, *and* $Ds_{20\text{-}80}$) between reference ground motions and replicas, as shown in Figure 10, indicates that the calibration procedure results in synthetic replicas with significant durations that are close to the reference ones. In general, the significant duration of the replicas oscillates around the reference values. However, in some cases, specifically for the highest magnitude group, the replicas exhibit durations that are either smaller or larger than the reference values. These divergences may be attributed to effects related to the specific path taken by seismic waves from source to site, specific source mechanisms not fully captured by a magnitude-based clustering, or the limitations in the adequacy of the modulating function model used for simulations in this application.

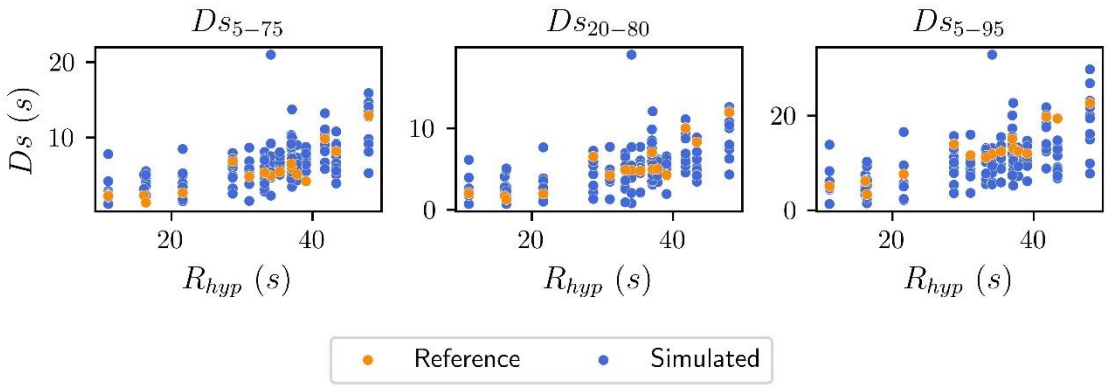

Figure 10: Comparison of three different durations (*Ds5-95, Ds5-75, and Ds20-80*), as a function of hypocentral distance, for the mid- magnitude earthquakes. The Y-axis of each plot represents each significant duration *Ds5-95, Ds5-75, and Ds20-80*, for the left, mid, and right panels.

5. Simulated ground motions and record selection for METIS case study

5.1 Synthetic database

The calibrated SGMSM can be employed to generate simulated ground motions that are consistent with those recorded in region of interest, at least in terms of the IMs considered in the calibration procedure. To illustrate the use of the calibrated SGMSM, a simulated database (referred to as SDB) was generated. The SDB consists of 4873 3D acceleration time histories, generated by simulating earthquake scenarios sampled from a uniform magnitude distribution ($4 \leq M_w \leq 6$) and within a maximum hypocentral distance of 60 km. These causative parameters were selected to be consistent with the disaggregation of the hazard at the site of the case study detailed in the report "MS7: PSHA output for METIS case study" (Chartier et al., 2023). The database follows a typical flat file structure, where each line represents a simulated ground motion, and each column contains features of the simulation. The following are the columns included in the presented database:

Parameter	key	units
Moment magnitude	mw	
Hypocenter depth	z	km
Hypocentral distance	r_hyp	km
Time step	dt	s
Acceleration time history for component *i**	acc_i	g
Pseudo Spectral acceleration at for component *i* period of vibration *T*[1]	saT_i	g
Arias Intensity for component i	ia_i	g/s
Significant duration between 5% and 95% IA for component i	sd595_i	s
Significant duration between 5% and 75% IA for component i*	sd575_i	s
Significant duration between 20% and 80% IA for component i	sd2080_i	s
Cumulative absolute velocity for component i*	cav_i	g*s

Table 1. Information included in the database*: *i* represents the component, 1 for North-South, 2 for East-West, and 3 for vertical. The components are, 1: NS, 2: EW, 3: UD and GM, which represents the geometrical mean of the horizontal components.

The time histories included in the SDB were generated using the same event-based approach described in section 4.5: i) a finite rupture model was generated for each sampled earthquake scenario, ii) a source spectrum was computed with the stress drop estimated for this application, iii) the source spectrum was then then attenuated, according to equation (6), to virtual stations located at different azimuths and distances (randomly sampled) from the assumed hypocenter of the rupture model. Once again, no site-effects were considered in the representation of the FAS because the objective of this application is to generate reference acceleration ground motion for site specific analysis. Figure 11 shows the attenuation of three different spectral amplitudes (PSA = 50 Hz (PGA), 5 Hz, and 1 Hz) for all simulated ground motions in the SDB.

[1] The period of vibration is represented in seconds. The periods of vibration included in the database are 0.01 (PGA), 0.05, 0.1, 0.2, 0.3, 0.4, 0.5, 0.75, 1.0, 1.6, 2.0, 4.0, 5.0, 8.0, 10.0s

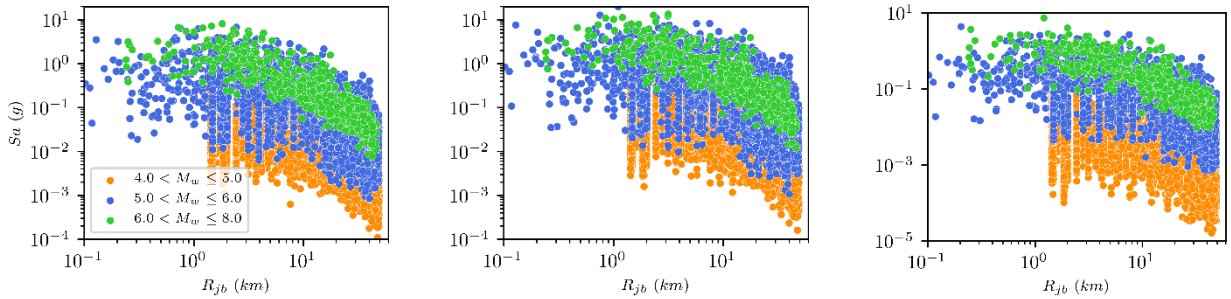

(a) (b) ©

Figure 11: Attenuation of the spectral accelerations of the events populating the SDB at different periods of vibration: (a) 50 Hz (PGA), (b) 5 Hz, and (c) 1.0 Hz.

A comparison of the attenuation of the spectral, for two different magnitude bins, and three periods of vibration, is shown in Figure 11. The figures shown the spectral acceleration from: i) the SDB (marked as simulated), ii) the recorded reference ground motions (marked as recorded), and iii) the predictions given by the ergodic application of the GMMs considered in the PSHA computations for the case study (Chartier & Rood, 2023). These models include the ESHM20 (Kotha et al., 2020) and the modified model reported by Lanzano (2019), derived for Italy, and adjusted to include the reference rock correction factor described in Lanzano et al., (2022). The results shown in the figure indicate that the spectral acceleration of the simulated ground motions matches that of the recorded ones in most cases. The largest differences were found in the lowest frequency (1 Hz) and for the higher magnitude bin. These differences were expected because of the discrepancies identified in the calibration procedure (see Figure 9) and are mostly attributed to the simplified assumptions regarding rupture and wave propagation considered in the stochastic ground motion simulation models, (Akazawa, et al., 2023). Furthermore, the differences may be due to the lack of recorded scenarios to exploit as training data for target scenarios with these causative parameters. This magnitude bin and frequency of vibration (largest magnitude and lowest frequency of vibration) also result in the largest discrepancies between simulated ground motions and predictions from the reference GMMs. In fact, apart from this specific case of lowest magnitude bin and longest period of vibration the comparison with respect to the GMMs was found to be rather good. A closer comparison, showing the distribution of spectral accelerations for a source-to-site distance of 40 km ($R_{jb} = 40\ km$), corresponding to the same magnitude bins and frequencies of vibration can be seen in the results shown in Figure 13. This specific distance was chosen due to the large amount of recorded data considered in the calibration of GMMs, thus allowing for a more realistic comparison of dispersion between the distributions. The results indicate that distributions of spectral accelerations from simulated ground motions are comparable to those of the ergodic application of the reference GMMs, specifically in the higher frequency range.

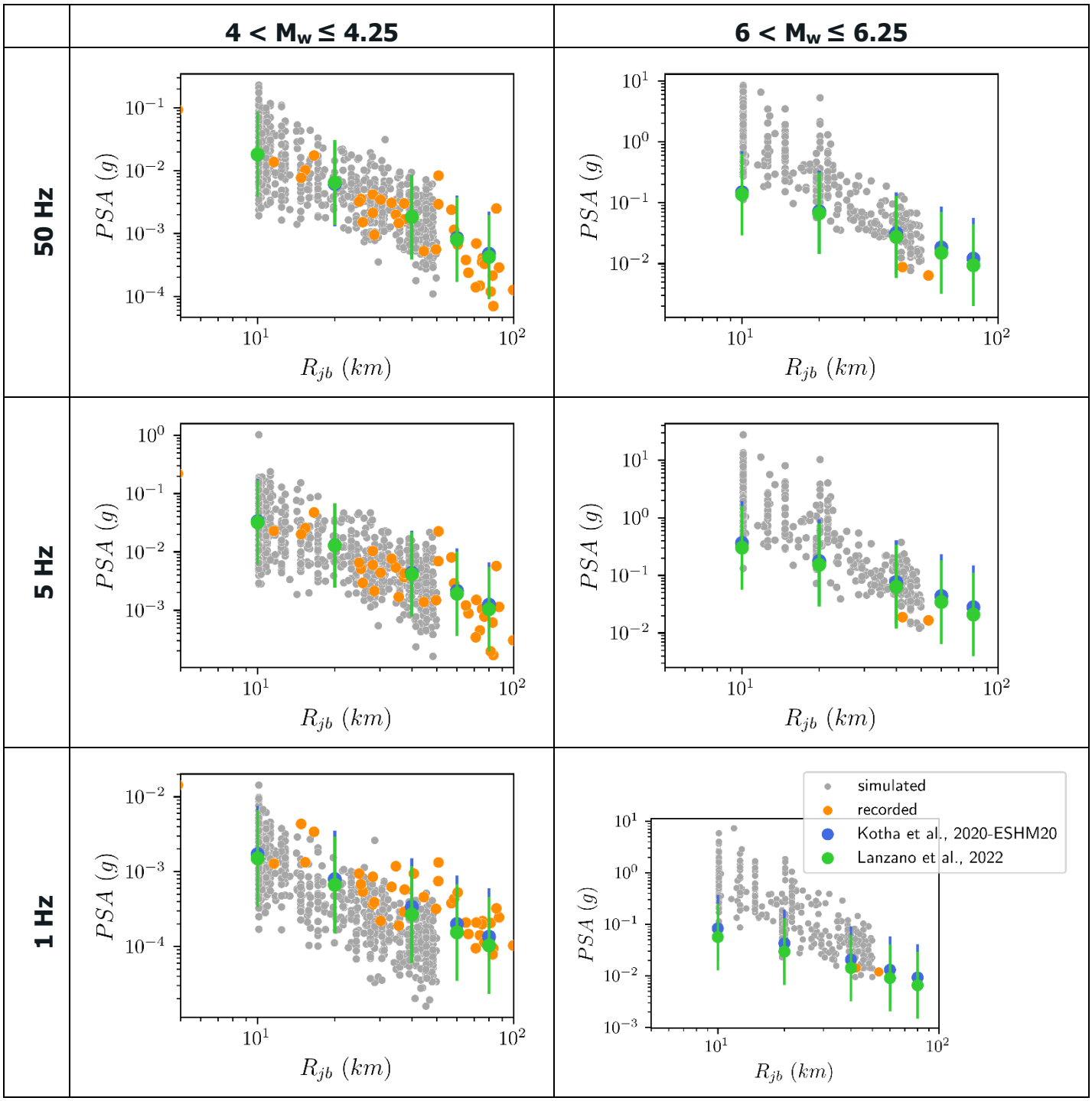

Figure 12: Comparison of the attenuation of the spectral accelerations for the RotD50 component (at different frequencies of vibration) of the events populating the SDB, and the recoded reference events. The figure includes also the estimations given by the ESHM20 (Kotha et al., 2020) and the modified Lanzano et al. (2022) ground motion models, here the marker signals the medium and the bars the intervals between the 5th-95th percentiles.

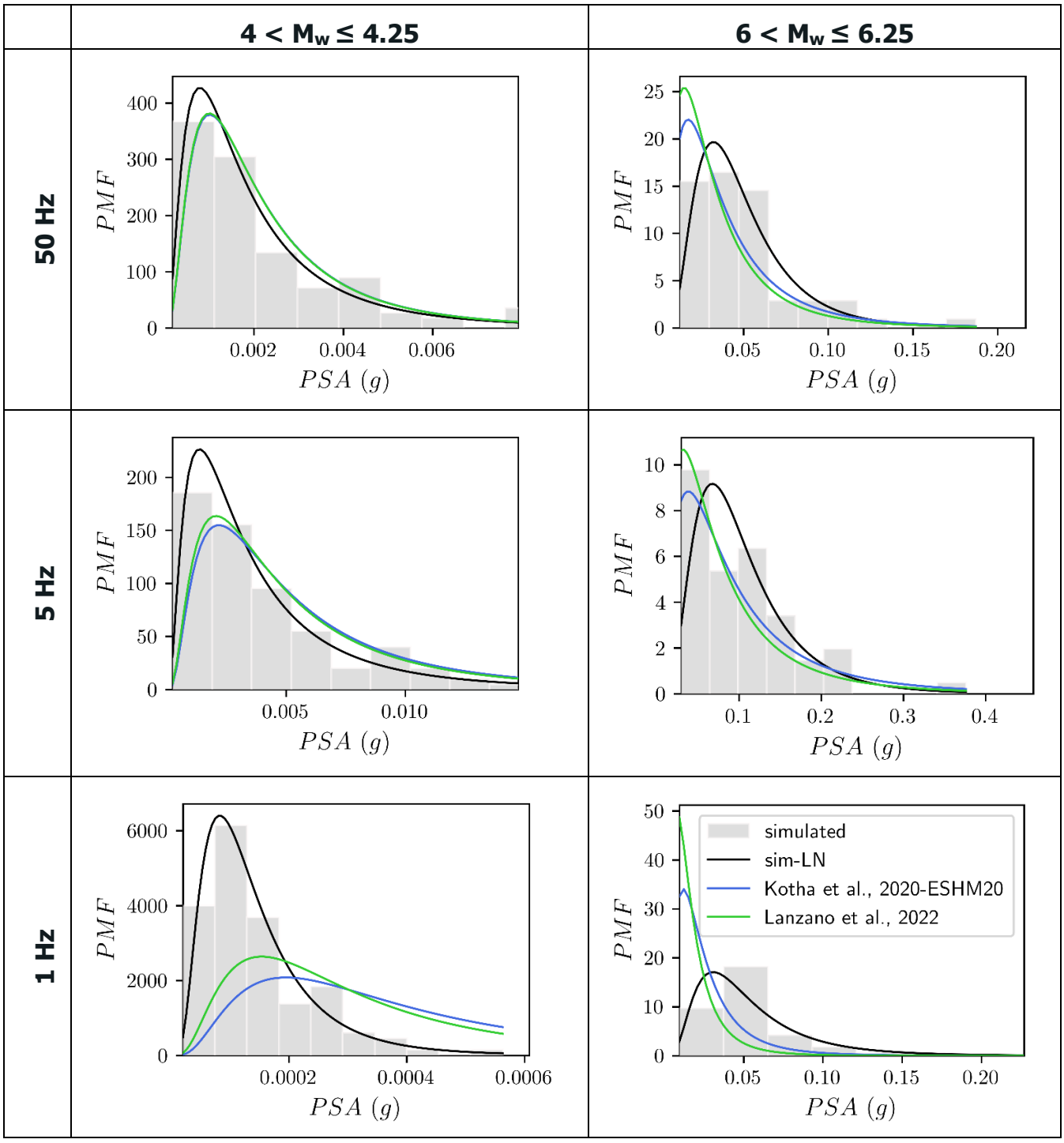

Figure 13: Comparison of distributions of spectral accelerations for the RotD50 component (at different periods of vibration and for a source to site distance of 40 km) of the events populating the SDB (histogram), a fitted log normal distribution for the distribution of the simulated ground motion (sim-LN), the recoded reference events, and the estimations given by the ESHM20 (Kotha et al., 2020) and the modified Lanzano et al. (2022) ground motion models. Here the Y-axis refers to the Probability Mass Function (PMF)

Finally, Figure 14 shows the comparison of the significant durations considered in the calibration of the SGMSM (*$Ds_{5\text{-}95}$, $Ds_{5\text{-}75}$, and $Ds_{20\text{-}80}$*). Overall, the results show the coherence between the significant durations of the simulated ground motions, those of the reference ground motions, and those predicted by the ground motion model proposed in Afshari & Stewart (2016).

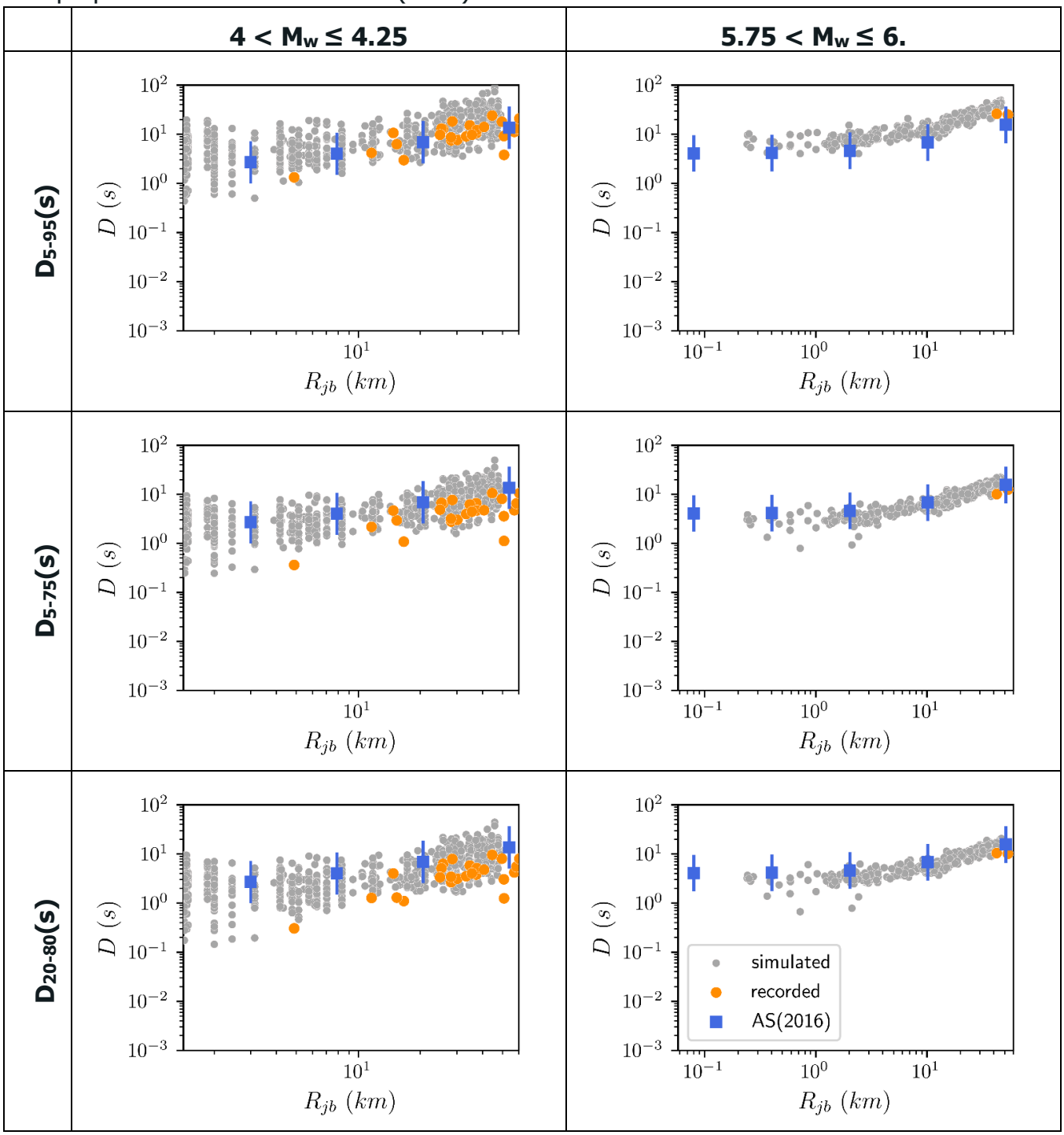

Figure 14: Comparison of the evolution of three different Significant durations for the GM component (*$Ds_{5\text{-}95}$, $Ds_{5\text{-}75}$, and $Ds_{20\text{-}80}$*), as a function of source-to-site distance, of ground motions populating the SDB, the reference ground motions, and the ground motion model proposed in Afshari & Stewart (2016), here referred to as AS(2016).

5.2 Record selection

The simulated ground motion database presented in this document was used for record selection based on the conditional spectra (CS) approach.

The conditional spectra were computed through the open-source software OpenQuake (Pagani M, 2014). for the site-specific PSHA model that was developed for the METIS case study (see METIS D4.6), and incorporating the new features included specifically for this application (see METIS D4.4). The underlying definition of the CS and the record selection procedures are the ones reported in (Lin, Harmsen, Baker, & Luco, 2013). More details on CS-based record selection procedures can be found in METIS D5.1.

Here, the record selection based on the conditional spectra approach was applied to the synthetic database developed for METIS and described in this report. The development of a regional model and consideration of specific scenarios allow for the selection procedure without additional constraints on distances or Vs30 values.

In comparison, the same record selection strategy was then applied to the ESM database (Luzi, et al., 2016). The conditioning IMs are the PGA and PSA (0.2s) (that is PSA at 5Hz) in both cases.

Definition of the target hazard

The CMS (Conditional Mean Spectra) and the Uniform Hazard Spectra (UHS) for METIS case study site are shown in Figure 15 (left) below. We consider 6 return periods corresponding to 500, 2500, 50000, 10000, 20000 and 50000 years, respectively. Figure 15 (right) shows the CMS together with the $\pm 1\sigma$ intervals. All conditional spectra have been defined as rotd50 values.

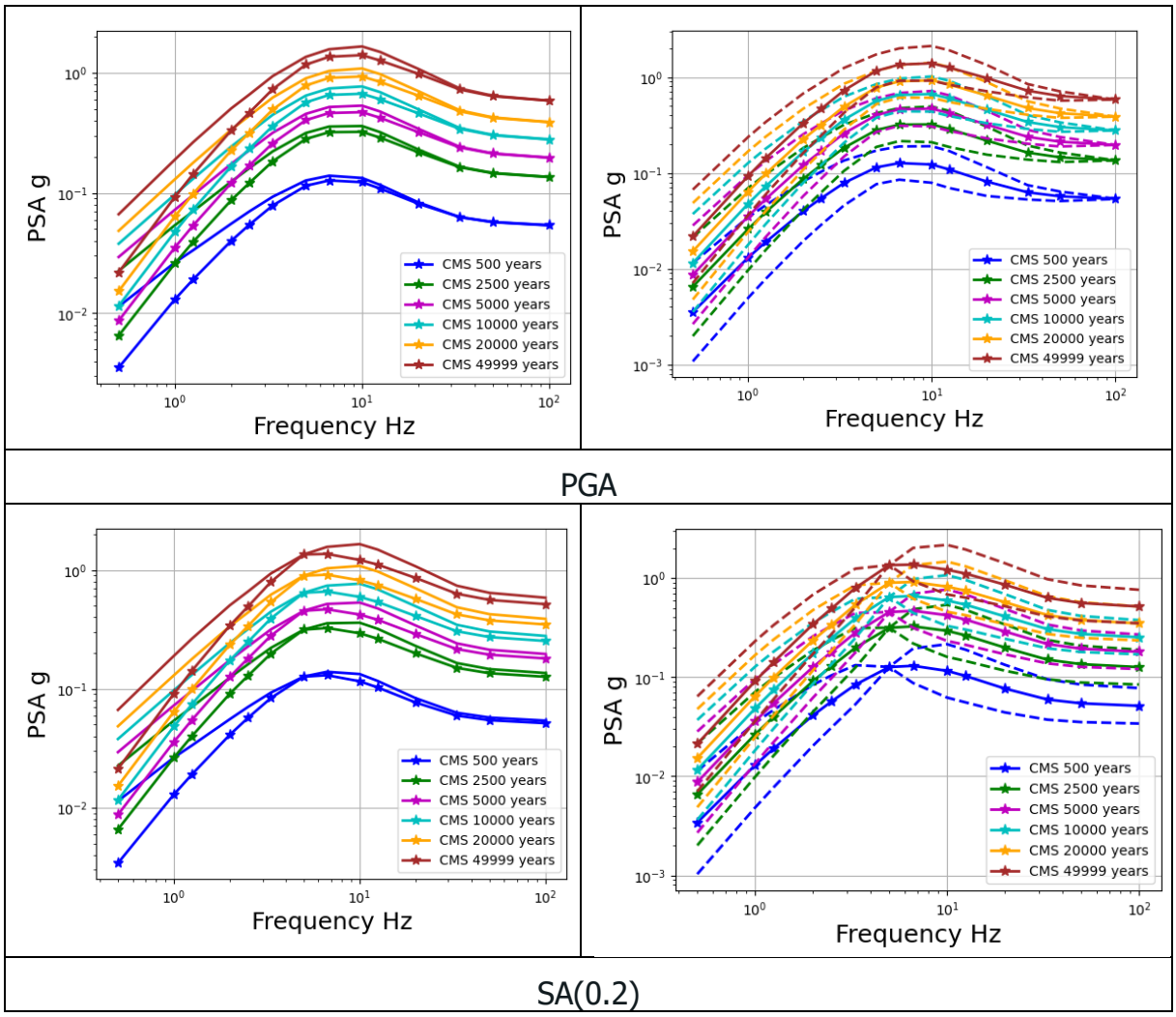

Figure 15: UHS and CMS (dashed line + stars) - (left) and CMS (solid lines) together with ±1σ intervals (dashed lines) - (right) for the two conditioning IMs PGA and SA(0.2). Data values where the CMS are computed are highlighted by stars in all figures.

Record selection for the synthetic database

The magnitudes of the 4873 time histories contained in the synthetic database are shown in Figure 16. The range of magnitudes considered for the record selection was slightly reduced to better comply with the major scenarios computed from METIS case study. Only magnitudes greater than 4.5 were accepted for record selection, and scaling was allowed only within the range of 0.5 to 5.0. The following constraints were applied in the recorded database (ESM) selection procedure:

- Strong motion duration in the range of 2.0s to 20.0s
- Scaling within the range of 0.5 to 5.0
- Magnitude in the range of 4.5 to 6.5

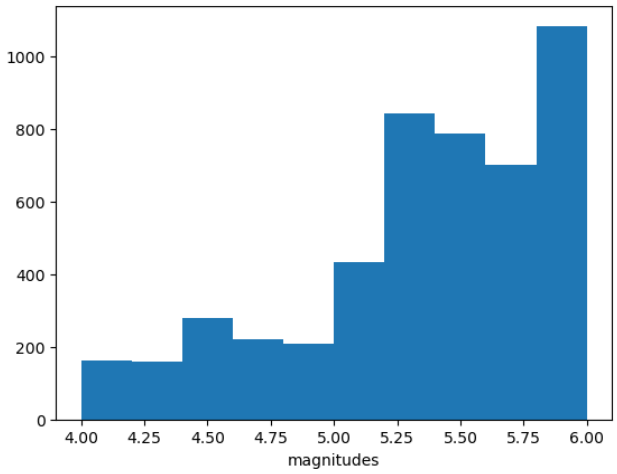

Figure 16: histogram of magnitude of the time histories in the synthetic database

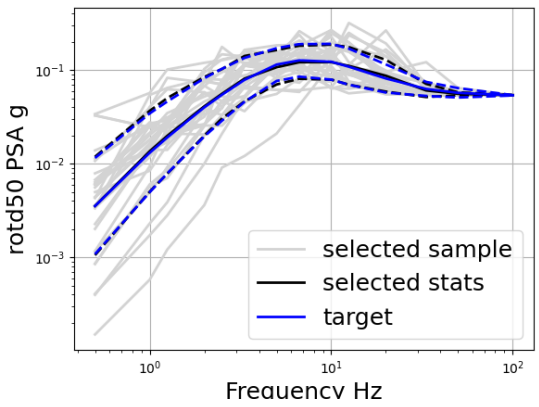

IML_1

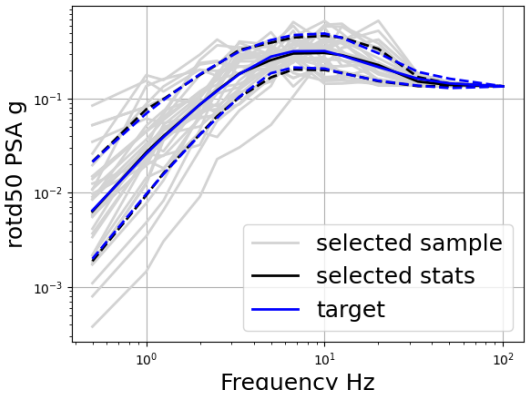

IML_2

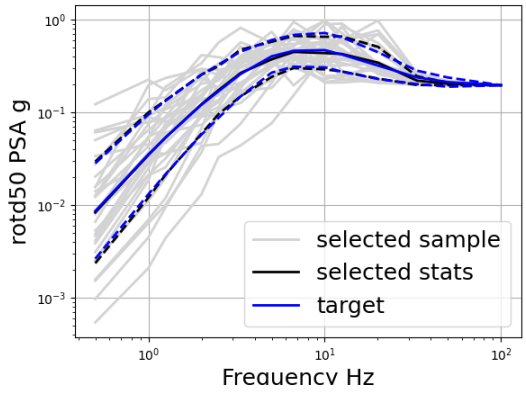

IML_3

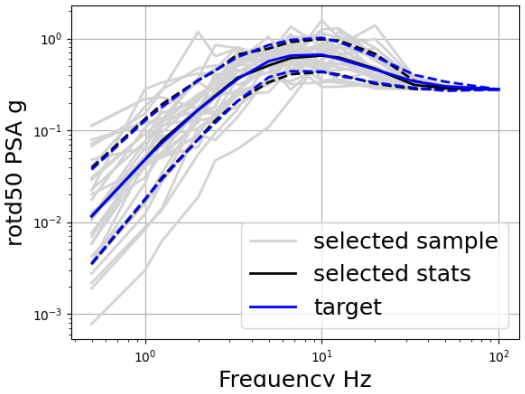

IML_4

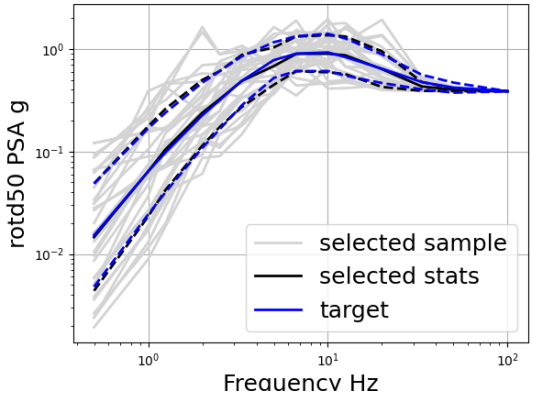

IML_5

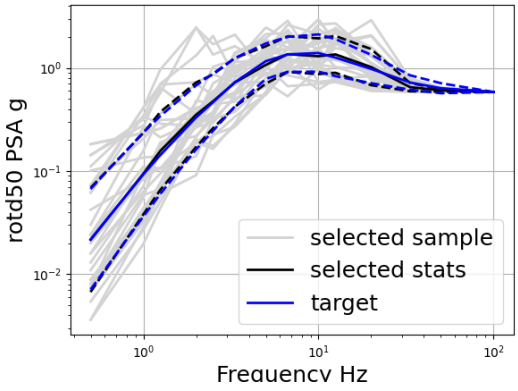

IML_6

Figure 17: PGA selection for synthetic database : Target spectra (blue) and selected response spectra (grey) with their statistics (black) for the 6 return periods (IML_1-IML_6) shown with increasing levels and for PGA as conditioning IM. The dashed lines are the ±1σ fractiles for the selected and the target spectra, respectively. IML_1to IML_6 are the different intensity levels corresponding to the 6 considered return periods.

Figure 17 shows the response spectra of the selected accelerograms together with their median and ±1σ intervals for comparison to the target. A very good fit is observed across most frequency, except for the very high frequency range between 50 and 100Hz where the target CS exhibit still non negligible variability, whereas simulated time histories all achieved constant spectral acceleration values. This is due to the simulation procedure with cut-off frequency <50Hz while the seismological ground motion models still predict evolution in frequency content. It has to be pointed out that given the usable frequency band of registrations, it is not sure whether this frequency content is physical or due to data processing issues in the records and derived GM models. The PSA(0.2s) selection shown in the Figure 18 is not impacted and has a good fit across all frequency ranges.

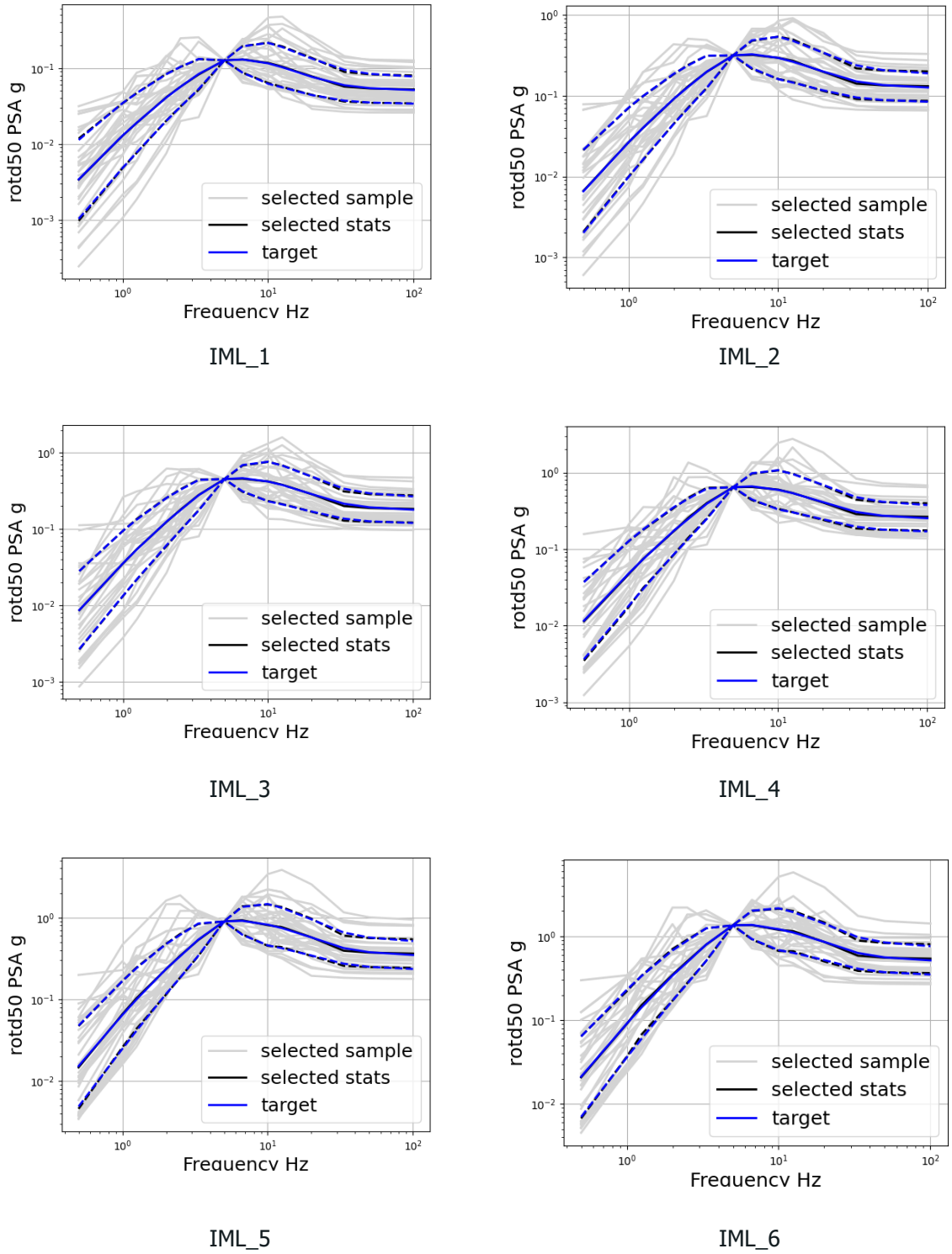

Figure 18: Sa(0.2) selection) selection for synthetic database: Target spectra (blue) and selected response spectra (grey) with their statistics (black) for the 6 return periods (IML_1-IML_6) shown with increasing levels and for PGA as conditioning IM.

Record selection for the ESM database

The results obtained with the synthetic database are then compared to the same record selection procedure applied to recorded accelerogram using the ESM database (Luzi et al 2020). In both cases the scaling factors (SFs) required to achieve good fit

were similar. In the past, the need for high scaling factors was mainly due to the limited number of signal available in the databases. However, modern databases like ESM contain many records allowing for the selection of a subset of admissible ground motions with requirements using the CS approach with limited scaling. The admissible range (0.5-5) works well for both synthetic and recorded database according to the studies conducted here.

For the case of PGA and PSA(0.2) selection, the scaling factors and sets of conditional spectra are compared in Figure 19. For comparison to Figure 17 and 18, the selection results are shown in Figure 20 for the ESM database. Spectral shapes of selected signal are in good agreement with the target likewise observed for the synthetic database. For the PGA selection, the records allow to represent the high frequency content predicted by the GMM.

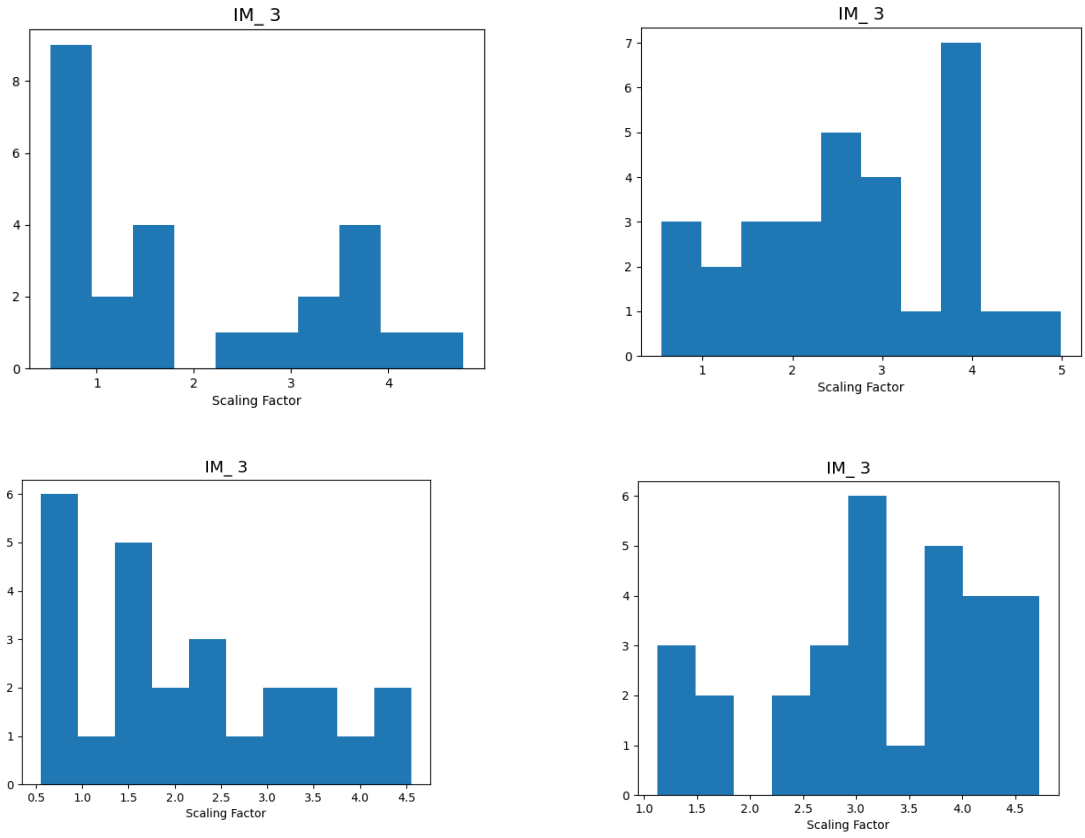

Figure 19: Histogram of scaling factors: comparison of selection results for the synthetic (left) and the recorded database (right) for PSA(0.2) (upper figures) and PGA (lower figures) for intensity level IM_3 (10 000 years return period).

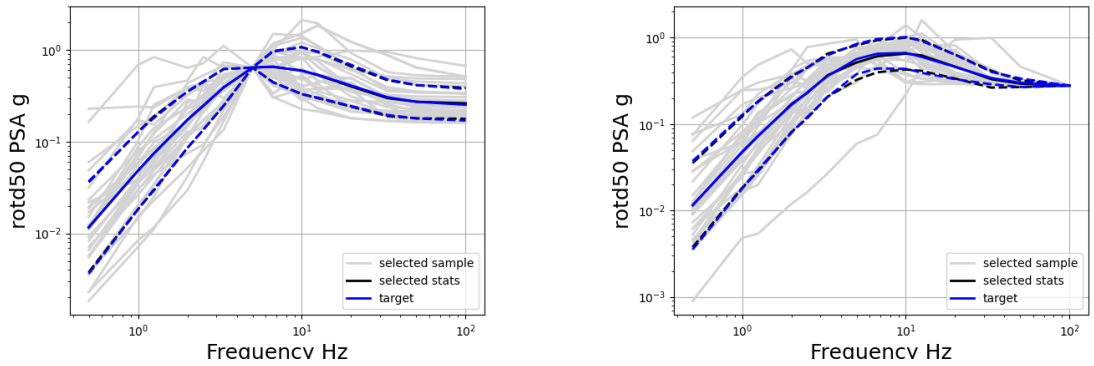

Figure 20: PSA(0.2) (left) and PGA (right) selection for ESM database: Target spectra (blue) and selected response spectra (grey) with their statistics (black) for 10 000 years return period.

The advantage of using a synthetic database is its possibility to generate acceleration time histories consistent with the source and propagation characteristics of the region and site of interest. Rock ground motions with Vs values larger than 1000m/s are still relatively scarce in the databases today but will certainly increase in future.

6. Supplementary materials

The data used for this study and the results are available through the following links.

- Database of simulated ground motions produced for the METIS case study: DOI 10.5281/zenodo.10692782.
- Target spectra used for the record selection: DOI 10.5281/zenodo.10664585.
- Set of synthetic records selected for METIS case study using the CS-approach: DOI 10.5281/zenodo.10925218.

References

METIS

Rood, A. (2024). METIS case study PSHA: openquake hdf5 output files for Conditional Spectra [Data set]. Zenodo. https://doi.org/10.5281/zenodo.10664586

Alvarez-Sanchez, L. (2024). METIS case study synthetic scenario ground motion database [Data set]. Zenodo. https://doi.org/10.5281/zenodo.10692783

Zentner, I. (2024). METIS case study record selection [Data set]. Zenodo. https://doi.org/10.5281/zenodo.10925219

METIS D4.6 - Preparation of the METIS hazard study case and application. Authors: Chartier, T., & Rood, A. (2024). Zenodo. https://doi.org/10.5281/zenodo.10529417

METIS D4.3 - Methodologies for physics-based simulation of ground motion. Analysis of different approaches and applications to METIS case study. Authors: Akazawa, T., Alvarez-Sanchez, L., Ameri, G., Baumont, D., Cotton, F., Irikura, K., Pilz, M., Razafindrakoto, H., Saint-Mard, L., Shible, H., Somei, K., & Zentner, I. (2023). Zenodo. https://doi.org/10.5281/zenodo.10397409

Other

Afshari, K., & Stewart, J. P. (2016). Physically Parametrized Prediction Equations for Significant duration in Active Crustal Regions. *Earthquake Spectra*, 32: 2057-2081.

Akazawa, T., Alvarez Sanchez, L., Ameri, G., Baumont, D., Cotton, F., Irikura, K., . . . Zentner, I. (2023). *Methodologies for physics-based simulation of ground motion: Analysis of different approaches and applications to METIS case study.* METIS.

Al Atik, L., Abrahamson, N., Bommer, J., & Kuehn, N. (2010). The variability of ground-motion prediction models and its components. *Seismological Research Letters*, 794-801.

Alvarez Sanchez, L. (2022). *Improved 3D Ground Motion Simulation for Structural Response Analysis.* Paris: Université Gustave Eiffel - Thesis.

Alvarez Sanchez, L., Quevedo de Inaritu, P., Sipcic, N., Kohrangi, M., & Bazzurro, P. (2023). Hazard-consistent simulated earthquake ground motions for PBEE applications on stiff soil and rock sites. *Earthquake Engineering & Structural Dynalics*, doi.org/10.1002/eqe.3987.

Anderson, J., & Hough, S. (1984). A MODEL FOR THE SHAPE OF THE FOURIER AMPLITUDE SPECTRUM OF ACCELERATION AT HIGH FREQUENCIES. *Bulletin*

of the Seismological Society of America, 74 (5): 1969–1993. doi: https://doi.org/10.1785/BSSA0740051969.

Baker, J. W. (2018). An Improved Algorithm for Selecting Ground Motions to Match a Conditional Spectrum. *Journal of Earthquake Engineering*, 22(4), 708–723.

Boore, D. (1983). Stochastic Simulation of High-Frequency Ground Motions based on Seismological Models of the Radiated Spectra. *Bulletin of the Seismological Society of America*, 73(6).

Boore, D. (2005). On pads qnd filters: Processing strong motion data. *Bulletin of the Seismological Society of America*, 95(2); 745-750. https://doi.org/10.1785/0120040160.

Brune, J. (1970). Tectonic Stress and the Spectra of Seismic Shear Waves from Earthquakes. *Journal of Geophysical Research*, 75: 4997-5009 - doi:10.1029/JB075i026p04997 .

Chartier, T., & Rood, A. (2023). *MS7: PSHA output for METIS case study.* METIS.

Cornell, A. (1968). Engineering seismic risk analysis . *Bulletin of the Seismological Society of America*, 1583-1606.

Gallovič, F. (2016). Modeling velocity recordings of the mw 6.0 south napa, California, earthquake: Unilateral event with weak high-frequency directivity. *Seismological Research Letters*, 87(1): 2–14. DOI: 10.1785/0220150042.

Garcia de Quevedo, P., Sipcic, N., Alvarez Sanchez, L., Kohrangi, M., & Bazzurro, P. (2023). A closer look at hazard-consistent ground motion record selection for building-specific risk assessment: Effect of soil characteristics and accelerograms' scaling. *Earthquake Spectra*, 1303-1327 doi.org/10.1177/87552930231187407.

Jayaram, N., & Baker, J. (2009). Correlation model for spatially distributed ground-motion intensities. *Earthquake Engineering and Structural Dynamics*, 1687-1708.

Kotha, S., Weatherill, G., Bindi, D., & Cotton, F. (2020). A regionally adaptable ground motion model for shaloow crustal earthquakes in Europ. *Bulletin of Earthquake Engineering*, 18: 4091-4125 - https://doi.org/10.1007/s10518-020-00869-1.

Lanzano G, S. S. (2019). The pan-European Engineering Strong Motion (ESM) flatfile: compilation criteria and data statistics. *Bulletin of Earthquake Engineering*, 17(2): 561-582 DOI: 10.1007/s10518-018-0480-.

Lanzano, G., Felicetta, C., Pacor, F., Spallarossa, D., & Traversa, P. (2022). Generic-To-Reference Rock Scaling Factors for Seismic Ground Motion in Italy. *Bulletin of the Seismological Society of America*, 112(3): 1583-1606.

Li, H., Michelini, A., Zhu, L., Bernardi, F., & Spada, M. (2017). Crustal velocity structure in Italy from analysis of regional seismic waveforms. *Bulletin of the Seismological Society of America*, (97). 2024-2039. DOI:10.1785/0120070071.

Lin, T., Harmsen, C., Baker, J., & Luco, N. (2013). Conditional Spectrum Computation Incorporating Multiple Causal Earthquakes and Ground Motion Prediction Models. *Bulletin of the Seismological Society of America* , 103 (2A): 1103–1116. doi: https://doi.org/10.1785.

Luzi, L., Puglia, R., Russo, E., D'Amico, M., Felicetta, C., Pacor, F., . . . Costa, G. (2016). The European strong-motion database: A platform to access accelerometric data. *Seismological Research Letters*, 87, no. 4 doi:https://doi.org/10.1785/0220150278.

Morasca, P., D'Amico, M., Sgobba, S., Lanzano, G., Colavitti, L., Pacor, F., & Spallarossa, D. (2023). Empirical corrzlations between an FAS non-ergodic ground motion model and a GIT derived model for Central Italy. *Geophysical Journal International*, 233, 51-68.

Otarola, C., & Ruiz, S. (2016). Stochastic generation of accelerograms for subduction earthquakes. *Bulletin of the Seismological Society of America*, 106(6): 2511-2520 - https://doi.org/10.1785/0120150262.

Oth, A., Parolai, S., & Bindi, D. (2011). Spectral analysis of K-NET and KiK-net data in Japan, Part I: Database compilation and peculiarities. *Bulletin of the Seismological Society of America*, 101(2), 652–666. https://doi.org/10.1785/0120100134.

Pagani M, M. D. (2014). OpenQuake Engine: An Open Hazard (and Risk) Software for the Global Earthquake Model. *Seismological Research Letters*, 85(3): 692–702. DOI: 10.1785/0220130087.

Ruiz, S., Ojeda, J., Pastén, C. O., & Silva, R. (2018). Stochastic strong-motion simulation in borehole and on surface for the 2011 m w 9.0 tohoku-oki megathrust earthquake considering p, sv, and sh amplification transfer functions. *Bulletin of the Seismological Society of America*, 108(5), 2333–2346. https://doi.org/10.1785/0120170342.

Saragoni, R. G., & Hart, G. C. (1973). Simulation of Artificial Earthquakes. *Earthquake Engineering and Structural Dynamics*, 2, 249-267.

Sipčič, N., Garcia de Quevedo Inarritu, P., Alvarez-Sanchez, L., M, K., & Bazzurro, P. (2021). *Methodology for site-specific rock-hazard_consistent record selection for mainshock-only siesmicity.* Pavia: METIS.

Steidl, J., Tumarkin, A., & Archuleta, R. (1996). What is a reference site? *Bulletin of the Seismological Society of America*, 86(6): 1733-1748.

Zentner, I. (2020). *D1.1 - Detailed WorkPlan.* Paris: EDF.